Study of the Coke Distribution in MTO Fluidized Bed Reactor with MP-PIC Approach

Xiaoshuai Yuan [ID],[1,2] Hua Li,[1] Mao Ye[1,*] and Zhongmin Liu[1]

1. Dalian National Laboratory for Clean Energy, National Engineering Laboratory for MTO, Dalian Institute of Chemical Physics, Chinese Academy of Sciences, Dalian 116023, China

2. University of Chinese Academy of Sciences, Beijing 100049, China

The methanol to olefins (MTO) process has received considerable interest due to its importance in transforming abundant resources such as coal, natural gas, and biomass to widely-demanded light olefins. In the MTO process, the coke deposited on the catalyst governs the catalyst activity and product selectivity, and thus is critical to the reaction behaviour. In the industrial processes, the residence time and coke content of catalyst particles in the reactor show a certain distribution due to the continuous outflow of spent catalyst and inflow of regenerated catalyst, which need further attention. The multi-phase particle-in-cell (MP-PIC) approach was used in the current work to simulate the catalyst residence time and coke content distribution. The effect of gas-solid flow patterns, reactor structure, and average catalyst residence time on the residence time and coke content distribution was investigated. It was found that at high superficial velocities, the coke content distributions obtained with the MP-PIC method are consistent with the distribution deduced from the ideally mixed flow assumption of catalyst particles. The results suggested that it is possible to simulate large-scale MTO reactors by use of the coke distribution. In particular, by incorporating an initial coke distribution, the time needed to reach steady state in the MTO reactor simulations could be greatly reduced.

Keywords: MTO, coke distribution, fluidized bed, CFD, MP-PIC

INTRODUCTION

The methanol to olefins (MTO) process has recieved extensive research since its discovery, and considerable efforts have been devoted to industrializing the technology. In 2010, the world's first commercial MTO unit was started in Baotou, China.[1] The unit was based on the MTO technology developed by the Dalian Institute of Chemical Physics (DICP), Chinese Academy of Sciences, namely the DMTO technology. In the DMTO process, the circulating fluidized bed (CFB) is adopted. However, the transportation of catalyst between the reactor and the regenerator causes the mixing of catalyst with a different residence time. For the MTO process, coke accumulates on catalyst particles with reaction time, and thus catalyst residence time has a significant effect on the coke content deposited on the catalyst. A wide distribution of catalyst residence time causes a wide distribution of coke content. Since the amount of coke deposited on the catalyst dominates the catalyst activity and product selectivity, research on catalyst coke distribution is very important in optimizing the design and operation of MTO reactors.

In the open literature, various reactor and kinetic models have been proposed to simulate the MTO fluidized-bed reactor. Bos et al.[2] proposed a lumped kinetic model and studied various types of reactors with the model. For the simulation of CFB reactors, Bos et al. suggested that the gas phase could be assumed to be in plug-flow and the solids to be ideally mixed. By relating the coke content to the residence time, the coke distribution could be calculated. However, the catalyst residence time is calculated based on the ideally mixed assumption, which should be further validated.

The computational fluid dynamics (CFD) calculations could obtain more detailed information about the reactor, and have recieved growing interest in recent years. Chang et al.[3]

investigated the effect of operation parameters on the MTO reaction by integrating a reaction model with a two-fluid model (TFM). It was found that the initial coke content on the catalyst plays a critical role in methanol conversion. The MTO reactor in their simulation was operated under fast fluidization conditions, and thus the amount of coke deposited on the catalyst was small. Therefore, the authors did not discuss the coke distribution in the reactor. Zhao et al.[4] simulated a large-scale MTO fluidized bed reactor (FBR) by using TFM, and a reaction model was implemented to test the model approach. Since the coke formation process was not included in the reaction model, the model could not reflect the effect of coke on the reaction. Zhu et al.[5,6] simulated the same MTO reactor by incorporating a filtered drag model to TFM. The effectiveness of the sub-grid models at coarse-grid conditions was validated with coke flow simulations, and then the model was used to simulate the MTO reaction behaviour. Based on the simulations, an optimum catalyst residence time and average coke content was proposed. Zhu et al.[7] further coupled the filtered CFD method with the population balance model to investigate the effect of particle polydispersity on the MTO process. The model could provide detailed information regarding particle breakage. However, the influence of coke distribution on the MTO reaction behaviour still needs to be investigated.

Considering that the formation of coke and its concentration are critical to methanol conversion and product selectivity in the

MTO process, the time-dependent coking behaviour is favoured in the simulation. However, due to the high demand on computation time and power, the time-dependent CFD simulation remains a great challenge. Lu et al.[8,9] combined the classic chemical reaction engineering (CRE) models and CFD approaches to speed up the time-dependent CFD simulation. The continuous stirred tank reactor (CSTR) model was used to estimate the steady-state distribution of coke content, and the results were set as the initial condition for the CFD simulation with TFM. However, the CSTR model gave a homogeneous distribution of coke content, which might not be the same as with the actual MTO reactors. The simulation results showed a large deviation from the experimental data, and the different coke distribution profile might be the reason for this deviation. In a recent work, Zhang et al.[10] further developed the model, and considered the initial coke distribution in the model. The simulation showed a better prediction of the experimental results. The results suggested that the coke content distribution is important in the simulation of the MTO process. However, the coke content distribution in the reactor is not thoroughly investigated in open literature.

For the simulation of coke distribution, the individual catalyst particles should be tracked to obtain detailed information regarding coke distribution. The discrete element method (DEM) is useful in the tracking of particles.[11–15] With the combined CFD-DEM model, the properties of particles could be simulated, and thus the coke distribution could be calculated. Zhuang et al.[16] simulated a laboratory-scale FBR with the combined CFD-DEM model. The coke formation and the real-time particle activity were calculated in the model. However, the authors did not consider the circulating of catalyst particles, and thus the coke distribution was not discussed. The multi-phase particle-in-cell (MP-PIC) approach is another method for tracking particles.[17,18] This approach allows for the calculation of inter-particle collisions by using a continuum description of the particle stress, and thus reduces the computation time significantly. The increased computational efficiency makes it suitable for large-scale FRB simulations. The MP-PIC approach has been recently applied to the simulation of large-scale fluidized catalytic cracking (FCC),[19] biomass-sand fluidized bed,[20] biomass-steam gasification,[21] etc. Therefore, the MP-PIC methodology is suitable for the simulation of industrial processes due to the enhanced computational efficiency.

In the current work, the MP-PIC approach implemented in OpenFOAM[22] was modified to simulate the age distribution in a FBR. The effect of gas-solid flow patterns, reactor structure, and average residence time on the catalyst residence time was investigated and compared with the calculations derived from the completely mixed flow model. Furthermore, the formation of coke was incorporated in the model and it was shown that the coke distribution is critical in the simulation of the MTO process.

MODEL DEVELOPMENT

For the simulation of dense gas-solid flow, the four-way coupling approach regarding the interaction between the gas and the particles is required, where both the interactions between the particles and the gas phase, and the inter-particle collisions should be considered. In the current work, the four-way coupling solver *MPPICFoam* implemented in OpenFOAM was modified to incorporate the formation of coke. To reduce the computational efforts, incompressible flow was assumed, and the corresponding governing

equations were given in this section. In addition, the formation of coke was also simplified, and will be discussed herein.

Continuum Phase

The multi-phase particle-in-cell method assumes an incompressible fluid phase with the corresponding continuity equation:[18,23]

$$\frac{\partial \alpha_f}{\partial t} + \nabla \cdot (\alpha_f \boldsymbol{u}_f) = 0 \tag{1}$$

where α_f is the fluid volume fraction, and $\boldsymbol{u}_f$ is the fluid velocity. Momentum transport is given by the incompressible Navier-Stokes equation for laminar flow:

$$\frac{\partial \alpha_f \boldsymbol{u}_f}{\partial t} + \nabla \cdot (\alpha_f \boldsymbol{u}_f \boldsymbol{u}_f) = -\frac{\nabla p}{\rho_f} + \alpha_f \boldsymbol{g} + \nabla \cdot \alpha_f \boldsymbol{\tau}_f - \frac{\boldsymbol{F}}{\rho_f} \tag{2}$$

where p is the fluid pressure, ρ_f is the fluid density, $\boldsymbol{g}$ is gravity, $\boldsymbol{\tau}_f$ is the stress tensor, and $\boldsymbol{F}$ is the momentum transfer term.

The stress tensor $\boldsymbol{\tau}_f$ is given by:

$$\boldsymbol{\tau}_f = \nu_f \left[\nabla \boldsymbol{u}_f + (\nabla \boldsymbol{u}_f)^T \right] - \frac{2}{3} \nu_f (\nabla \cdot \boldsymbol{u}_f) \boldsymbol{\delta} \tag{3}$$

where ν_f is the kinematic viscosity (defined as $\frac{\mu_f}{\rho_f}$), μ_f is the dynamic viscosity, and $\boldsymbol{\delta}$ is the unit tensor.

In OpenFOAM, the interphase momentum transfer term $\boldsymbol{F}$ is decomposed to the adjusted drag and a local acceleration term:[22,24]

$$\boldsymbol{F} = \frac{1}{V_c} \sum_p \left[\beta (\boldsymbol{u}_f - \boldsymbol{u}_p) - \rho_f V_p \left(\boldsymbol{g} - \frac{D\boldsymbol{u}_f}{Dt} \right) \right] \tag{4}$$

where $\boldsymbol{u}_p$ is the particle velocity, and β is the drag force coefficient. Note that the drag force coefficient β calculated in OpenFOAM is also adjusted, and thus includes both the drag and the effect of relative motion on the local pressure gradient.

Particulate Phase

The particle phase is governed by the probability distribution function (PDF), $\phi(\boldsymbol{x}, \boldsymbol{u}_p, \rho_p, V_p, t)$, and is described by the equation:[18]

$$\frac{\partial \phi}{\partial t} + \nabla \cdot (\phi \boldsymbol{u}_p) + \nabla_{\boldsymbol{u}_p} \cdot (\phi \boldsymbol{A}_p) = \frac{\phi_G - \phi}{\tau_G} \tag{5}$$

where $\nabla_{\boldsymbol{u}_p}$ is the divergence operator with respect to velocity, and $\boldsymbol{A}_p$ is the particle acceleration. $\boldsymbol{A}_p$ is defined as:

$$\boldsymbol{A}_p = \frac{d\boldsymbol{u}_p}{dt} = \frac{\beta}{m_p} (\boldsymbol{u}_f - \boldsymbol{u}_p) - \frac{\rho_f}{\rho_p} \left(\boldsymbol{g} - \frac{D\boldsymbol{u}_f}{Dt} \right) + \boldsymbol{g} - \frac{\nabla \tau_p}{(1 - \alpha_f) \rho_p} \tag{6}$$

Karimipour and Pugsley[25] investigated the effect of drag models in the simulation of bubbling fluidized beds with the MP-PIC method, and it was found that the choice of drag models has a minor effect on the model results. Therefore, the ErgunWenYu-Drag model, which was used by Karimipour and Pugsley, was incorporated in the current work to calculate the drag force coefficient β. The model is an implementation of the Ergun, Wen, and

Yu drag models in OpenFOAM, and is described by the following equations:[22]

$$\beta = \begin{cases} \left(150\dfrac{1-\alpha_f}{\alpha_f} + 1.75Re_p\right)\dfrac{\mu_f}{\alpha_f d_p^2}V_p & (\alpha_f < 0.8) \\ 0.75C_dRe_p\alpha_f^{-2.65}\dfrac{\mu_f}{d_p^2}V_p & (\alpha_f \geq 0.8) \end{cases} \tag{7}$$

$$C_d = \frac{24}{\alpha_f Re_p}\left[1 + 0.15(\alpha_f Re_p)^{0.687}\right] \tag{8}$$

$$Re_p = \rho_f d_p \frac{|u_f - u_p|}{\mu_f}. \tag{9}$$

The particle stress τ_p is calculated with the modified Harris and Crighton model:[18]

$$\tau_p = \frac{P_s\alpha_p^b}{\max\left[\alpha_{cp} - \alpha_p, \epsilon\left(1 - \alpha_p\right)\right]} \tag{10}$$

where α_{cp} is the close-pack volume fraction, α_p is the particle volume fraction, and $\alpha_p = 1 - \alpha_f$. P_s, b, and ϵ are constants. According to the suggestions by Snider et al.[18,26] and Hernández et al.,[24] the values of P_s, b, and ϵ are set to 10 Pa, 2, and 10^{-8}, respectively.

The right hand side of Equation (5) represents the collisional return-to-isotropy force. In OpenFOAM, a stochastic return-to-isotropy model is implemented.[22] The stochasitic model describes the relaxation of particle velocity distribution towards an isotropic Gaussian distribution (ϕ_G). τ_G is the relaxation time. The detailed explanation of the model could be found in O'Rourke and Snider's publications.[27,28]

Coke Formation Model

For the MTO process, the coke deposited on the catalyst dominates the catalyst activity and product selectivity, and thus a kinetic model that captures both the main reaction and the deactivation process is of industrial importance. Recent studies suggest that the MTO process follows the dual-cycle mechanism,[29] where the main products are formed via both the olefins-based and the aromatics-based cycle. According to this mechanism, the deactivation process could be considered to follow the transformation of active hydrocarbon species to heavy inactive species. Most of the kinetic models proposed focus on the main reaction.[30–34] The reason might be that the effect of coke on the reaction results is not straightforward in a fixed bed reactor since the catalyst bed features an inhomogeneous distribution.[35–37] However, the coke distribution in a laboratory-scale FBR can be assumed to be uniform due to the excellent back mixing of the catalyst.[37,38] Thus, it could be used to evaluate the catalyst performance and determine the effect of coke.

In our recent work, an MTO kinetic model was established based on the experimental results in a laboratory-scale FBR. Based on the model, the coke deposition rate could be expressed as:

$$R(c_c) = \frac{dc_c}{dt} = k_d(c_c^{max} - c_c) \tag{11}$$

where c_c is the coke content of the catalyst particle (dimensionless), and c_c^{max} is the maximum coke content (dimensionless). k_d is the coke deposition rate constant (s^{-1}), which is related to the concentration of methanol and major products. In the kinetic model, the deactivating effect of coke on catalyst activity ϕ could be represented with the following equation:

$$\phi = \frac{\exp\left[-\left(\dfrac{c_c^{max} - c_c^{cri}}{c_c^{max} - c_c}\right)^5\right]}{\exp\left[-\left(\dfrac{c_c^{max} - c_c^{cri}}{c_c^{max}}\right)^5\right]} \tag{12}$$

where c_c^{cri} is the critical coke content (dimensionless). From the equation, it could be found that the relationship between the catalyst activity and the coke content is nonlinear, and thus needs further attention in the simulation of the MTO process.

To reveal the coke distribution profile in the reactor, the time-dependent coking behaviour should be simulated. In the MTO process, the average catalyst residence time in the reactor is about 1 h.[1] To achieve a steady coke distribution, the simulation time should be much longer than the average residence time, which is on the order of several hours. Considering the current computing capability, a time-dependent simulation remains a great challenge. Therefore, some simplifications should be made to realize the time-dependent simulation.

In the current work, it is found that the effect of the coke deposition rate constant and average catalyst residence time on coke distribution is coupled, and their product is the dominating factor that determines the coke distribution. Therefore, the coke deposition rate constant k_d was adjusted, so that the simulation time could be reduced. Moreover, a CFB reactor was simulated, so the methanol and product distribution in the reactor is constant during steady state operation. Thus, the coke deposition rate k_d is also a constant, and is set to 0.1 s^{-1}. The corresponding average catalyst residence time is also changed so that the product of k_d and τ keeps close to that of the actual MTO process. The value of τ is determined by the number of particles in the bed and the catalyst inflow rate, where the former is kept constant and the latter is changed to give different values of τ. The obtained values of τ are about 3, 5, 10, 20, and 30 s, respectively. In this way, the effect of catalyst residence time and coke deposition rate on the coke distribution could be investigated. The detailed discussion will be given in the Results and Discussion.

MODEL SET UP AND PARAMETERS

The simulations were preformed in a 3D FBR. Compared to the industrial MTO reactors, the reactor structure was simplified and the reactor dimensions were reduced to achieve an efficient simulation. The computational conditions and parameters are given in Table 1. Three different mesh sizes, 0.5, 1, and 2 mm, were used to examine the mesh dependency. The superficial velocities of 0.05, 0.10, 0.20, and 0.35 m/s were used to investigate the different flow patterns. Different dimensions of the fluidized bed were used to reduce computation efforts under low superficial velocities and ensure full fluidization under high superficial velocities. When the superficial velocity U_0 = 0.05, 0.10, and 0.20 m/s, the height of the bed is 0.072 m; when the superficial velocity U_0 = 0.35 m/s, the height of the bed is increased to 0.144 m. The number of parcels in the simulation is about 180 000, and only one particle is considered in each parcel.

The effect of catalyst inlet and outlet structures was investigated by setting different patches as the catalyst inflow and outflow. The schematic representation of the inlet and outlet structures is shown in Figure 1. In a typical MTO fluidized bed reactor, catalyst particles flow into the reactor above the catalyst bed via the centre

Table 1. Computation conditions and parameters

Descriptions	Values
Geometry	Three-dimensional
Dimension	0.00075 m × 0.024 m × 0.072 m
	or 0.00075 m × 0.024 m × 0.144 m
Number of particles	~180 000
Particle diameter	100×10^{-6} m
Particle density	1520 kg/m^3
Solid fraction at maximum packing	0.60
Gas superficial velocity	0.05, 0.10, 0.20, 0.35 m/s
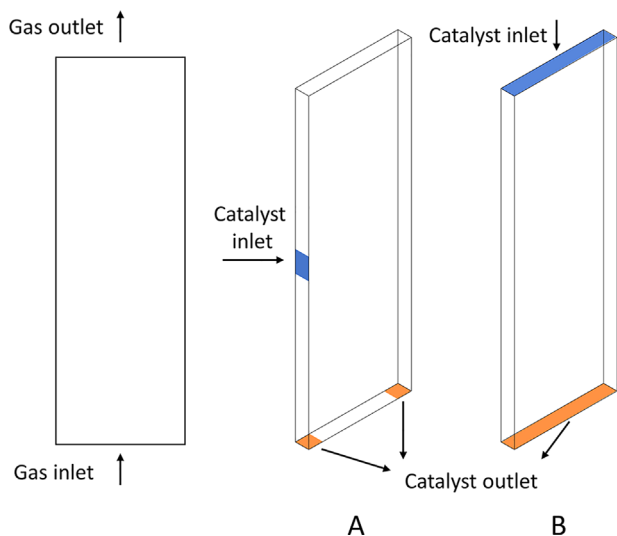
Figure 1. The schematic representation of the catalyst inlet and exit structures.

or one side of the reactor, and flow out of the reactor via the bottom. Therefore, structure A is adopted as an imitation of the MTO fluidized bed reactor, where catalyst particles flow into the reactor from the side and flow out from the bottom. Structure B is adopted to simulate a different catalyst back mixing pattern, where catalyst particles flow into the reactor from the top of the reactor and flow out from the bottom.
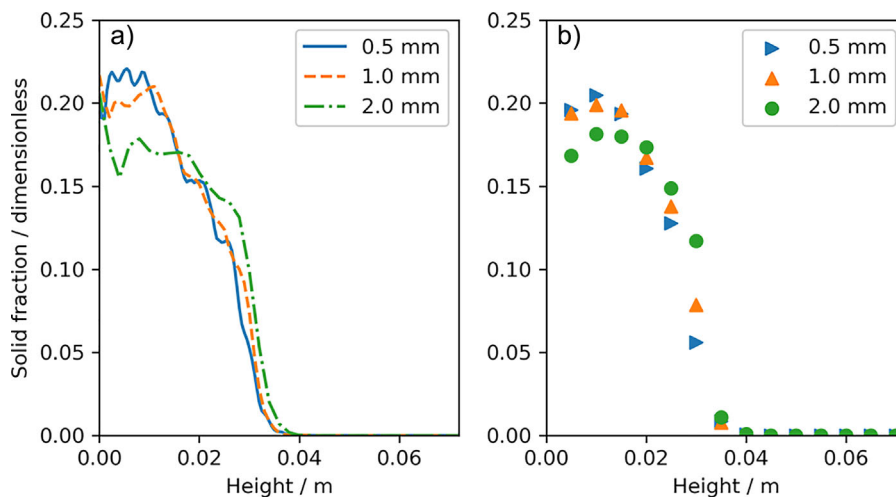
The gas phase enters the fluidized bed from the bottom of the bed and exits from the top of the bed. At the gas phase inlet, the *interstitialInletVelocity* boundary condition was specified; at the outlet, the *pressureInletOutletVelocity* boundary condition was used; and the walls were specified as *noSlip* boundary condition. The *fixedFluxPressure* boundary condition was used for the pressure at the fluidized bed inlet and the walls, and the *fixedValue* boundary condition was employed at the bed outlet. The initial pressure in the bed was set to constant. For the particle phase, a modified *localInteraction* patch interaction model was applied. The particles rebound at the walls, as well as the gas inlet and outlet boundaries, with an elasticity coefficient *e* of 0.97, and a restitution coefficient *mu* of 0.09. At the catalyst outlet, a special boundary condition was implemented. When the number of particles in the bed exceeds a given value, particles disappear randomly at the catalyst outlet; when the number of particles is smaller than the given value, the boundary is the same with the walls and particles rebound to the catalyst bed. In this way, the number of particles in the bed was kept constant. The detailed explanation of these boundary conditions can be found in the OpenFOAM user guide.[22]

RESULTS AND DISCUSSION

Grid Sensitivity Examination

Three different uniform meshes were used to examine the mesh dependency. As shown in Figure 2, the mesh sizes are 0.5, 1.0, and 2.0 mm. Figure 2a shows the axial profile of the solid fraction at the cross-section centre, and Figure 2b shows the average axial profile over each cross-section. The simulations with different mesh sizes show that the solid fraction is almost uniform in the lower fraction of the bed, and a sudden decrease in solid fraction is observed at the higher fraction of the bed. However, the solid fraction predicted by the simulation with the mesh size of 2.0 mm is lower than the simulation results with the mesh sizes of 1.0 and 0.5 mm. The result indicates that the mesh sizes of 1.0 and 0.5 mm are suitable for this simulation. Therefore, the mesh size of 0.5 mm was selected in the current work.

Gas-Solid Flow Patterns

The gas-solid flow patterns may influence particle back mixing and internal circulation, and thus are important in the

Figure 2. Axial profile of solid fraction inside the fluidized bed: (a) solid fraction at the cross-section centre; and (b) average solid fraction for each cross-section. $U_0 = 0.2$ m/s, and the solid fraction was averaged over the time period 10-25 s.

investigation of catalyst residence time and coke distribution. The typical flow patterns under different superficial velocities are shown in Figure 3. Catalyst does not circulate in these simulations, and thus the particle inlet or outlet conditions are not set. When the superficial velocity U_0 is 0.05 m/s, a homogeneous fluidization is observed. The back mixing of catalyst particles only exists in a small range. As U_0 increases to 0.10 m/s, the fluidized bed expansion is more obvious, and both the dense phase and dilute phase could be observed in the catalyst bed. Compared with the homogeneous fluidization, the particle back mixing is enhanced. When U_0 is increased to 0.20 m/s, a typical annulus-core structure is observed. The phenomenon is more obvious when the superficial velocity is further increased. With the annulus-core structure, the particle backing mixing is quite strong.

Catalyst Residence Time Distribution

The effect of various operation conditions on catalyst residence time distribution was simulated to investigate the catalyst back mixing in a circulating fluidized bed. The results were compared with the calculations from a CSTR model to show its deviation from the completely mixed flow. For a CSTR, the catalyst residence time distribution could be represented with the PDF:

$$p(t) = \frac{1}{\tau} \exp\left(-\frac{t}{\tau}\right) \tag{13}$$

where t is the catalyst residence time, and τ is the average catalyst residence time. For the simulation results, the histograms are used to show the catalyst residence time distribution. The histograms are normalized to form a probability density, and thus the simulation results and the calculation results from a CSTR model could be compared directly. Figures 4–6 show the influence of superficial velocities, catalyst inlet and outlet structure, and catalyst average residence time, respectively.

Figure 4 shows the catalyst residence time distribution with different superficial velocities and the comparision of simulation results with the calculation results from a CSTR model. As shown in the previous section, different flow strutures were observed under the simulated superficial velocities. The results in Figure 4 suggest that the deviation of catalyst back mixing from the completely mixed flow is quite significant under relatively low superficial velocities (U_0 = 0.05 and 0.10 m/s). The phenomenon is obvious since a low superficial velocity gives a less mixed flow structure. As the superficial velocity increases, the catalyst residence time distribution tends to a completely mixed flow. It should also be noted that when U_0 = 0.05 m/s, a small fraction of the catalyst particle shows quite a long residence time. The results indicate the existence of a dead zone in the reactor. When U_0 increases to 0.10 m/s, the deviation still exists, while the dead zone seems to disappear. Generally, the deviation of flow pattern from an ideally mixed flow causes a longer catalyst residence time.

The influence of catalyst inlet and outlet structure was also investigated. The comparison between Figures 4 and 5 shows the influence of catalyst inlet and outlet structure on the catalyst residence time distribution. For reactor structure A, catalyst particles flow into the reactor from the left side, and flow out
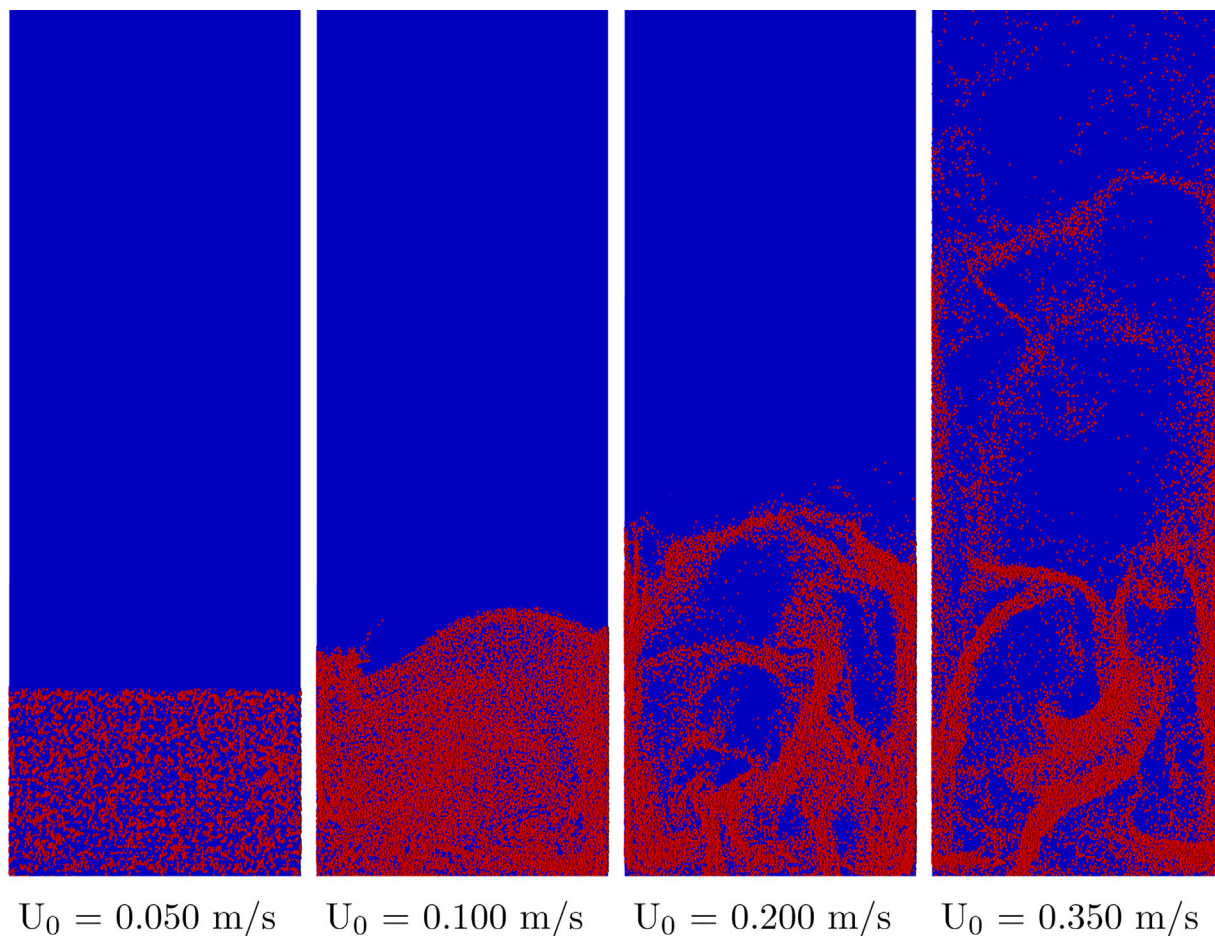

$$U_0 = 0.050 \text{ m/s} \quad U_0 = 0.100 \text{ m/s} \quad U_0 = 0.200 \text{ m/s} \quad U_0 = 0.350 \text{ m/s}$$

Figure 3. Gas-solid flow patterns with different superficial velocities.
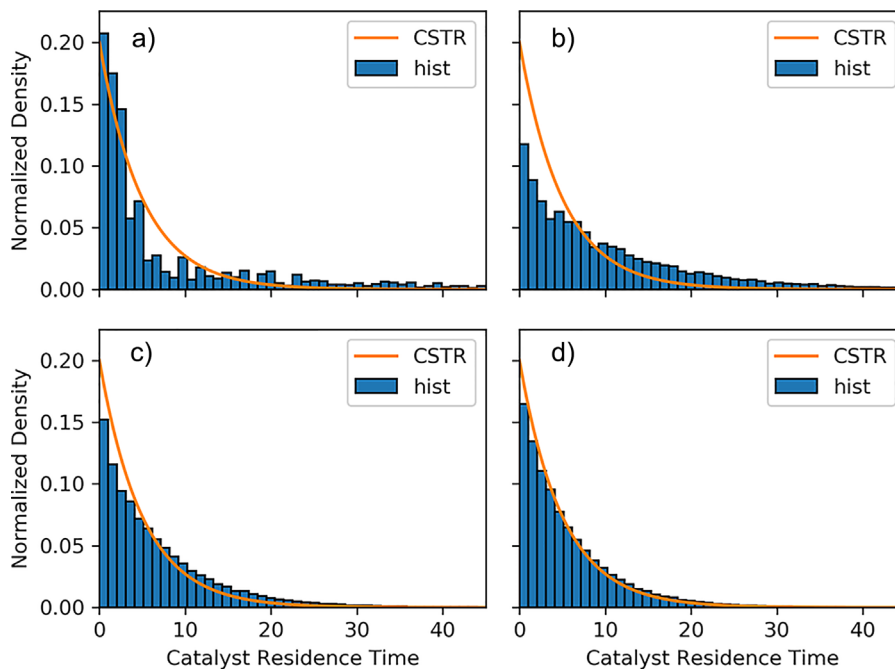
Figure 4. Catalyst residence time distribution with different superficial velocities: (a) $U_0 = 0.05$ m/s; (b) $U_0 = 0.10$ m/s; (c) $U_0 = 0.20$ m/s; and (d) $U_0 = 0.35$ m/s. $\tau = 5$ s.

via the corners at the bottom. While for structure B, catalyst particles flow into the reactor from the top and flow out from the bottom. With structure B, dead zones in the reactor should be eliminated. The results in Figure 5a suggest that, when the catalyst back mixing is not significant, the catalyst residence time distribution tends to the distribution in a plug flow. Comparing with structure A, no dead zone is observed under this reactor structure. The phenomenon is caused by a more homogeneous inlet and outlet of catalyst. As the superficial velocity increases, the catalyst residence time distribution is also closer to the results with a completely mixed flow. Note that when $U_0 = 0.35$ m/s,

the deviation between the simulation results and the calculation with a CSTR model is quite obvious. The results are caused by the gathering of catalyst particles at the top of the bed. As shown in Figure 3, a typical annulus-core structure is observed when $U_0 = 0.35$ m/s. The gas phase velocity is higher at the bed centre and becomes lower near the walls. Therefore, catalyst particles gathered at the top might flow down along the walls, thus causing a short catalyst residence time. The phenomenon could be avoided by adding an expanded section at the top part of the reactor.

Figure 6 shows the effect of average catalyst residence time on catalyst residence time distribution. The simulations were
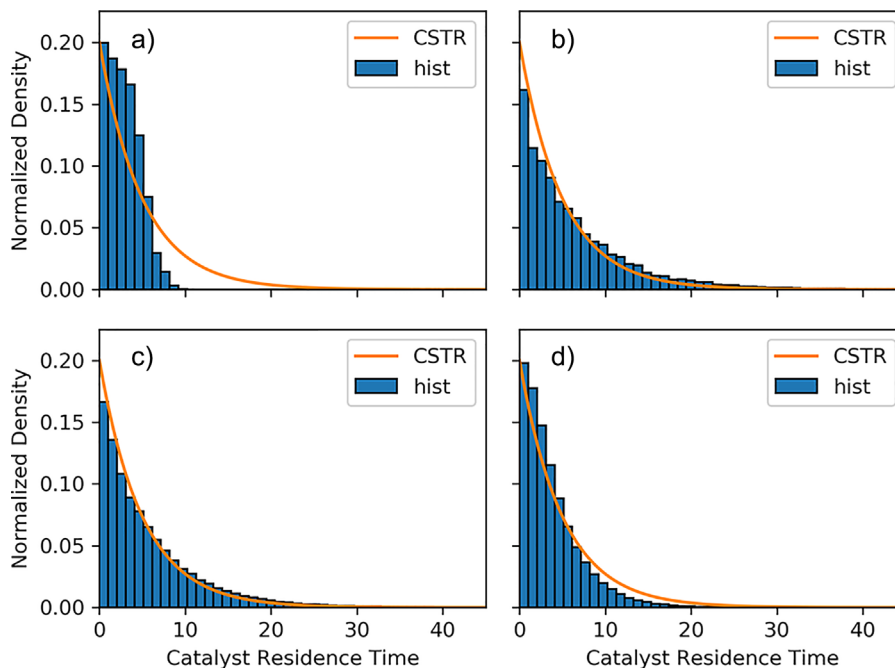

Figure 5. Catalyst residence time distribution with different superficial velocities: (a) $U_0 = 0.05$ m/s; (b) $U_0 = 0.10$ m/s; (c) $U_0 = 0.20$ m/s; and (d) $U_0 = 0.35$ m/s. $\tau = 5$ s.
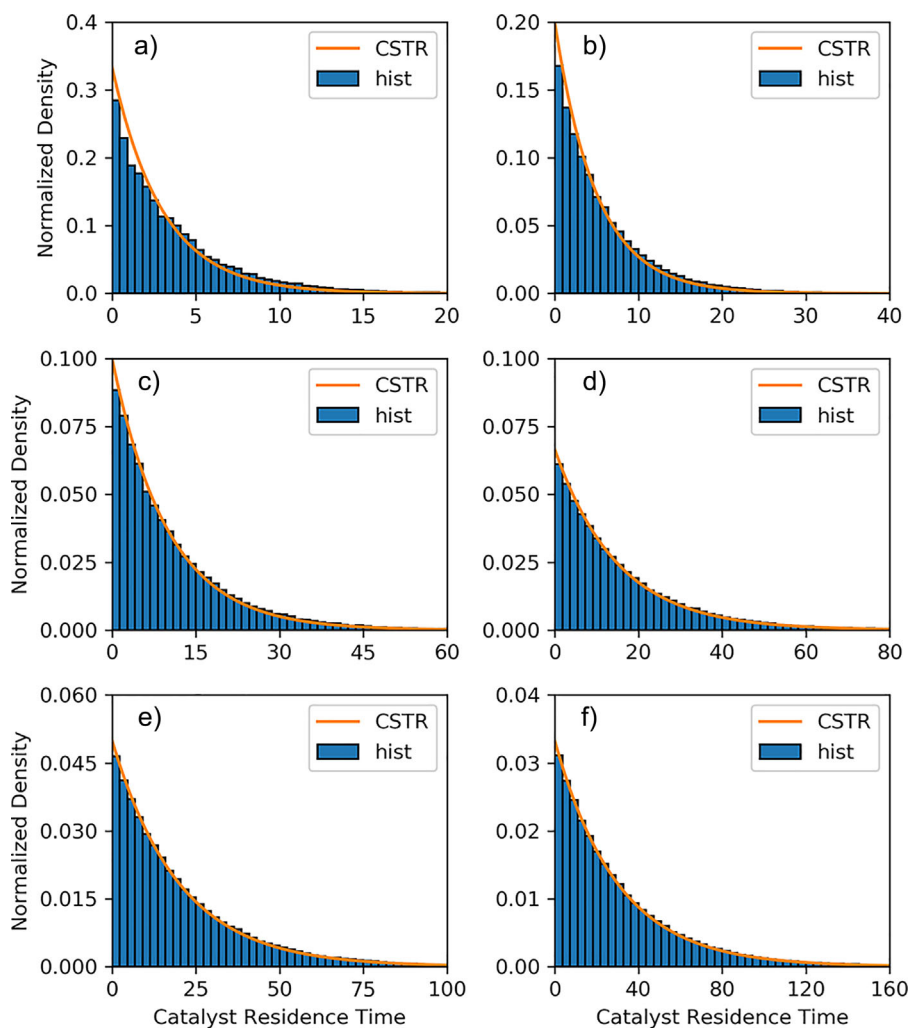
Figure 6. Catalyst residence time distribution with average residence time. $U_0 = 0.35$ m/s: (a) $\tau = 3$ s; (b) $\tau = 5$ s; (c) $\tau = 10$ s; (d) $\tau = 15$ s; (e) $\tau = 20$ s; and (f) $\tau = 30$ s.

conducted at the superficial velocity of $U_0 = 0.35$ m/s, and the reactor structure A, as shown in Figure 1, was used. The results show that the simulated coke distribution at low average residence time demonstrates a larger deviation with the distribution predicted with a CSTR model. The results indicate that the deviation of the simulated distribution with the CSTR model is related to the time scale of average residence time. Although the catalyst back mixing is quite strong at the simulated operation conditions, the flow could not be regarded as ideally mixed when catalyst particles circulate very fast. As shown in Figure 6, the catalyst particles tend to stay longer than the residence time predicted with the CSTR model. With the increase of average catalyst residence time, the catalyst residence time distribution is closer to the distribution with a CSTR model. In an industrial MTO process, the average catalyst residence time is much longer than the average catalyst residence time used in the current work. Moreover, turbulent fluidized bed reactors are used in the industrial MTO units, which exhibit better catalyst back mixing. Therefore, the modelling of CFB reactors in MTO industry could use the CSTR model to increase efficiency.

Catalyst Coke Distribution

In the kinetic studies, it is found that coke content is the key parameter that governs the catalyst activity and selectivity of the MTO reaction.[2,37,39,40] Therefore, the coke content distribution and its effect on the catalyst activity and product selectivity should be taken into consideration. From Equation (11), the relationship between c_c and t could be derived as:

$$c_c = c_c^{\max} - \exp\left(\ln c_c^{\max} - k_d t\right) \tag{14}$$

where the coke content is related to the residence time. Note that Equation (14) is used to calculate the coke content of a single particle. For a particle cloud, the individual particles may have different residence times. In a CSTR, catalyst particles are ideally mixed, and thus the residence time distribution could be represented with Equation (13). In this case, the residence time t is a variable with known distribution, and the coke content c_c is a function of the residence time t. Therefore, the PDF of coke distribution could be computed from Equations (13) and (14):

$$p(c_c) = \frac{1}{k_d \tau (c_c^{\max} - c_c)} \exp\left[\frac{1}{k_d \tau} \ln\left(1 - \frac{c_c}{c_c^{\max}}\right)\right]. \tag{15}$$

As the MP-PIC approach could track the individual particles, the coke distribution could also be simulated. The coke content was regarded as an addtional property of the particles and the feature was implemented in OpenFOAM. The simulation results are

presented in the form of histograms, which are also normalized as in the case of catalyst residence time. The comparison between the simulation results and the calculation results from Equation (15) is shown in Figures 7–9.

Figure 7 shows the coke content distribution and the comparison with a CSTR model. Comparing with the residence time distribution (see Figure 4), the deviation of flow pattern with a completely mixed flow causes a more significant deviation in coke content distribution. When $U_0 = 0.05$ m/s, due to the existence of the dead zone, the PDF of the coke content near the maximum coke content is quite large. When $U_0 = 0.10$ m/s, the simulation result also shows a high probability at high coke contents. For the simulation results with higher U_0 (0.20 and 0.35 m/s), the coke content distribution shows a similar trend with the calculation results from a CSTR model. As shown in Figure 4, the catalyst residence time is longer with a non-ideally mixed flow, thus resulting in a coke distribution with higher coke contents than the ideally mixed flow. Since the evolution of the coke formation rate with catalyst residence time is nonlinear, as shown in Equation (11), the influence of flow pattern on coke content and residence time distribution is different. It is obvious that the coke content distribution is more sensitive to the flow pattern changes.

The catalyst inlet and outlet structure also has a significant influence on coke content distribution. Figure 8 shows the simulated coke distribution with reactor structure B. As shown in Figure 5a, the catalyst inlet and outlet structure gives a short catalyst residence time at low superficial velocity. Thus, the short residence time leads to the coke distribution with a majority of low coke content, as shown in Figure 8a. As the superficial velocity increases, the coke content distribution tends to the results with a completely mixed flow. The phenomenon is caused by a more homogeneous inlet and outlet of catalyst. The gathering of catalyst at the top of the bed gives a coke distribution with more catalyst with low coke content, as shown in Figure 8d.

Figure 9 shows the effect of average catalyst residence time on the coke content distribution. The results suggest that the average catalyst residence time has a significant effect on the coke distribution. When the average catalyst residence time is smaller than 10 s, the coke content distribution tends to the distribution with a majority of low coke contents; when the average catalyst residence time is longer than 10 s, the coke content distribution tends to the distribution with a majority of high coke contents. In the current work, the average catalyst residence time of 10 s is a critical point where the coke content distribution is uniform. Note that in Equation (15), the influence of average catalyst residence time τ and coke deposition rate k_d is coupled together. The value of $\tau = 10$ s corresponds to the value of $k_d\tau = 1$. The results suggest that the value of $k_d\tau$ is a key parameter that determines the coke content distribution. In industrial practice, it is usually hard to determine the coke distribution. However, the average catalyst residence time is known, and the coke deposition rate could be determined in the kinetic studies. Thus, the parameter $k_d\tau$ could indicate the coke distribution in the industrial reactors. In the current simulations, the value of $k_d\tau$ was kept close to the corresponding $k_d\tau$ in the real MTO process, and thus the simulated coke distribution could reflect the real coke distribution in the industrial MTO reactor. The values of k_d and τ were changed accordingly to reduce simulation time.

The effect of inlet coke distribution was also investigated, as shown in Figure 10. In the simulations, the average coke content was kept constant (about 1.43 %), and four different distributions were considered, namely the single coke content of 1.43 %, the normal coke distribution with the standard deviation of 0.001, the normal coke distribution with the standard deviation of 0.005, and the exponential coke distribution. The superficial velocity is 0.35 m/s, and the catalyst average residence time is 15 s. Both the initial and the final coke distributions are shown in Figure 10. For the catalyst inlet with single coke content, as shown in Figure 10a, the coke distribution shifts to the higher coke contents. When the initial coke distribution is a little wider, the final coke distribution is only slightly different. However, the results in Figure 10c–d show an obvious difference since the initial coke distribution is much wider.
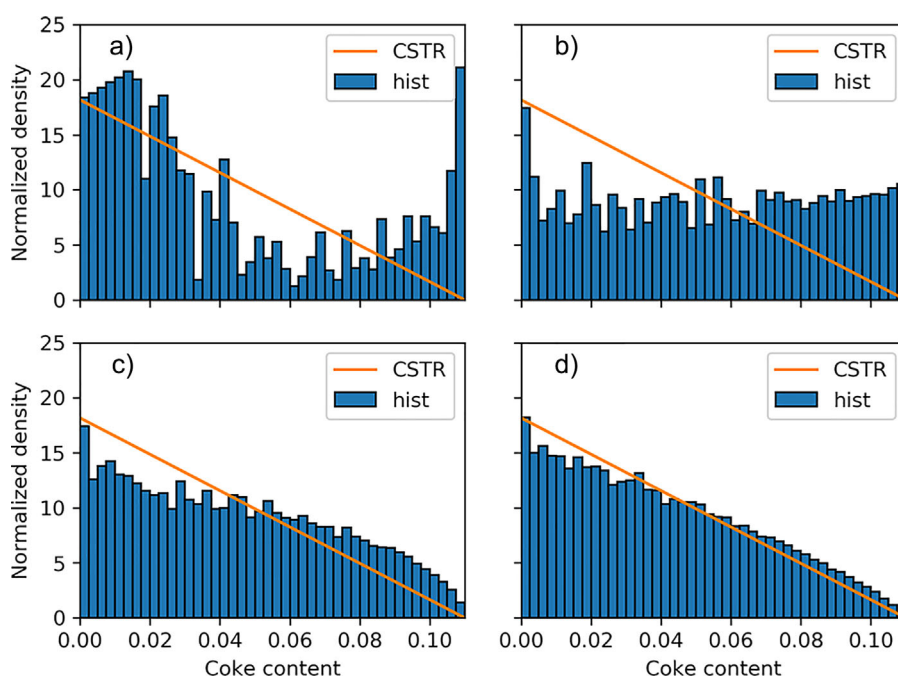

Figure 7. Catalyst coke distribution with different superficial velocities: (a) $U_0 = 0.05$ m/s; (b) $U_0 = 0.10$ m/s; (c) $U_0 = 0.20$ m/s; and (d) $U_0 = 0.35$ m/s. $\tau = 5$ s.
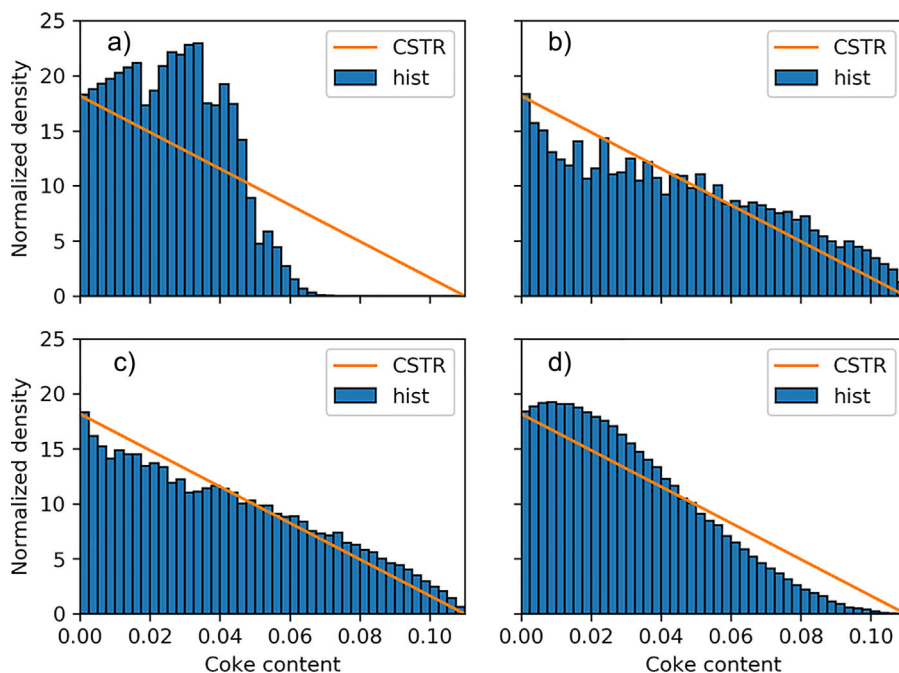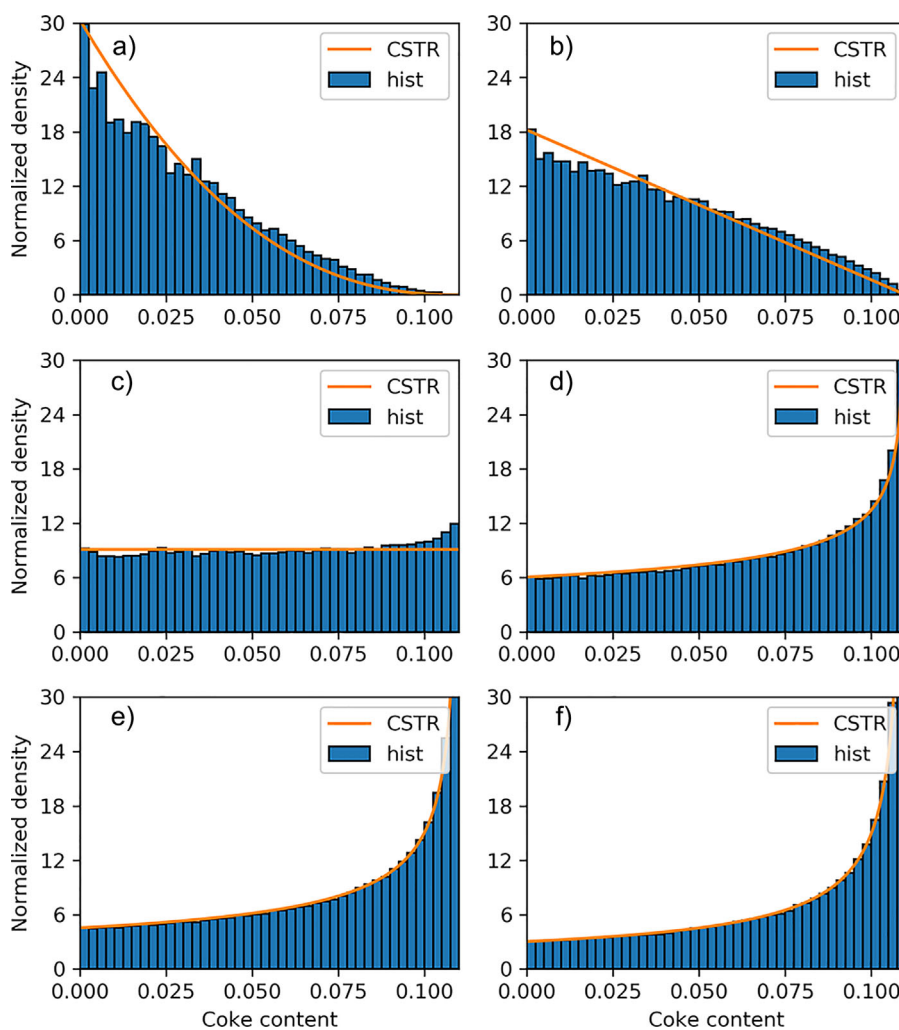
Figure 8. Catalyst coke distribution with different superficial velocities: (a) $U_0 = 0.05$ m/s; (b) $U_0 = 0.10$ m/s; (c) $U_0 = 0.20$ m/s; and (d) $U_0 = 0.35$ m/s. $\tau = 5$ s.

Figure 9. Catalyst coke content distribution with average residence time. $U_0 = 0.35$ m/s: (a) $\tau = 3$ s; (b) $\tau = 5$ s; (c) $\tau = 10$ s; (d) $\tau = 15$ s; (e) $\tau = 20$ s; and (f) $\tau = 30$ s.
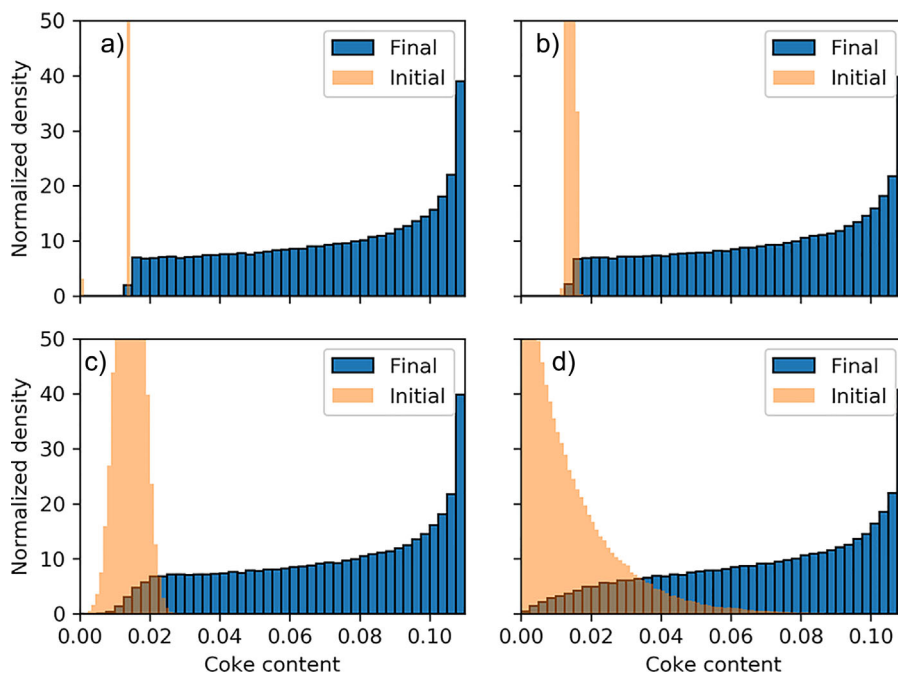
Figure 10. Effect of initial coke content distribution. $U_0 = 0.35$ m/s; $\tau = 15$ s: (a) single coke content at inlet; (b) normal coke content distribution (narrow) at inlet; (c) normal coke content distribution (wide) at inlet; and (d) exponential coke content distribution at inlet.

Due to the rapid deactivation of SAPO-34 catalyst, the fluidized bed reactor-regenerator configuration is adopted in the industrial process to allow for the in-line combustion of coke.[1] In this configuration, catalyst particles circulate between the reactor and the regenerator. The incomplete regeneration technology is adopted because an optimal amount of coke is beneficial to the MTO process. Therefore, the catalyst particles that flow out of the regenerator also have a coke distribution. As shown in Figure 10, different initial coke distributions result in different final coke distributions, thus leading to different reaction results. The effect of initial coke distribution would be more significant if the initial average coke content is larger. The results should be further incorporated with the kinetic model to reveal the effect of these distributions on the final reaction behaviour.

The coke content is critical in the MTO process, and the coke distribution should be taken into consideration in the simulation work. In a recent work, Zhang et al.[10] further developed the combined TFM and EMMS drag model proposed by Lu et al.,[8,9] and the coke content distribution was considered in the solid phase. They concluded that catalyst particles with low coke content have significant influence on the overall reaction behaviour, and thus the coke distribution rather than the average coke content should be considered in the simulation of the MTO process. The simulation results with coke distribution and its comparision with the previous model, as well as the experimental results are shown in Figure 11. It is shown that the discrepancy in the prediction of MTO reaction behaviour could be reduced by incorporating the coke distribution in the simulation. The conclusion is in accordance with the simulation results in the current work. It should be noted that the simulation in the current work is quite simplified, and further work is still needed to obtain a better understanding of the process. Nevertheless, the simulated coke distribution could be used as an initial condition for the simulation of MTO reactors, and thus reduce the time to reach steady state.
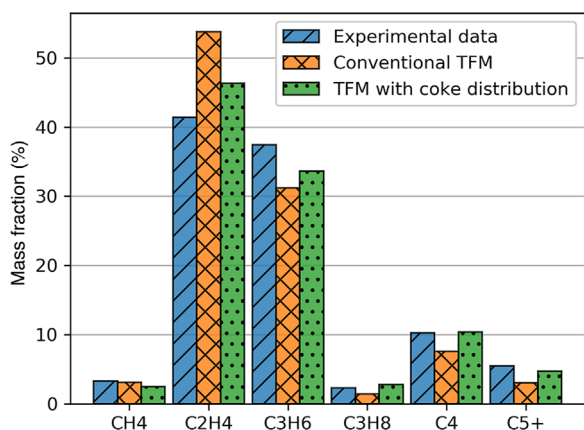
CONCLUSIONS

The coke deposited on the catalyst has a significant influence on the MTO performance over SAPO-34 catalyst, and an optimal amount of coke is favoured to increase the selectivity to light olefins. Therefore, the optimization of coke content distribution is quite important to improve the operation efficiency in the commercial MTO units. However, the coke content distribution could not be obtained directly from the experimental data, and thus simulations are often used to predict the coke content distribution. In the current work, the MP-PIC approach implemented in OpenFOAM was modified to simulate the coke distribution in circulating fluidized beds.

The gas-solid flow pattern has a great effect on the catalyst residence time and coke content distribution. At low superficial velocities, the back mixing of catalyst is not significant. Both the catalyst residence time and the coke content distribution show a large deviation from the completely mixed flow. With the increase

Figure 11. Mass fraction of gaseous product obtained from simulation and experiment. Reproduced from Zhang et al.[10]

of superficial velocities, both the catalyst residence time and the coke content distribution become closer to the completely mixed flow. The reactor structures also have an influence on the catalyst residence time and the coke content distribution. When the structure imitating the industrial MTO reactors is used, the catalyst residence time and the coke content distribution could be represented by the model derived from the completely mixed flow assumption of catalyst particles at high superficial velocities.

The average catalyst residence time and the initial coke content distribution are important parameters that determine the final coke content distribution. The effect of average catalyst residence time τ is coupled with the coke formation rate constant k_d. It is found that the parameter $k_d\tau$ could be used as an indicator for coke distribution in industrial MTO reactors and $k_d\tau = 1$ is a critical point. The catalyst particles tend to have a high coke content for $k_d\tau > 1$ and a low coke content for $k_d\tau > 1$. Different initial coke distributions will change the final coke distribution in the reactor. Thus, the regeneration process is also very important in the MTO process. However, it should be noted that the current model is simplified from the real industrial MTO process, and thus the influence of average catalyst residence time and initial coke distribution should be further validated. Nevertheless, the simulated coke distribution could be used to reduce the time to reach steady state in MTO reactor simulations.

ACKNOWLEDGEMENTS

REFERENCES

[1] P. Tian, Y. Wei, M. Ye, Z. Liu, *ACS Catal.* **2015**, *5*, 1922.

[2] A. N. R. Bos, P. J. J. Tromp, H. N. Akse, *Ind. Eng. Chem. Res.* **1995**, *34*, 3808.

[3] J. Chang, K. Zhang, H. Chen, Y. Yang, L. Zhang, *Chem. Eng. Res. Des.* **2013**, *91*, 2355.

[4] Y. Zhao, H. Li, M. Ye, Z. Liu, *Ind. Eng. Chem. Res.* **2013**, *52*, 11354.

[5] L.-T. Zhu, L. Xie, J. Xiao, Z.-H. Luo, *Chem. Eng. Sci.* **2016**, *143*, 369.

[6] L.-T. Zhu, M. Ye, Z.-H. Luo, *Ind. Eng. Chem. Res.* **2016**, *55*, 11887.

[7] L.-T. Zhu, H. Pan, Y.-H. Su, Z.-H. Luo, *Ind. Eng. Chem. Res.* **2017**, *56*, 1090.

[8] B. Lu, H. Luo, H. Li, W. Wang, M. Ye, Z. Liu, J. Li, *Chem. Eng. Sci.* **2016**, *143*, 341.

[9] B. Lu, J. Zhang, H. Luo, W. Wang, H. Li, M. Ye, Z. Liu, J. Li, *Chem. Eng. Sci.* **2017**, *171*, 244.

[10] J. Zhang, B. Lu, F. Chen, H. Li, M. Ye, W. Wang, *Chem. Eng. Sci.* **2018**, *189*, 212.

[11] N. G. Deen, M. Van Sint Annaland, M. A. Van der Hoef, J. A. M. Kuipers, *Chem. Eng. Sci.* **2007**, *62*, 28.

[12] H. P. Zhu, Z. Y. Zhou, R. Y. Yang, A. B. Yu, *Chem. Eng. Sci.* **2008**, *63*, 5728.

[13] Z. Y. Zhou, S. B. Kuang, K. W. Chu, A. B. Yu, *J. Fluid Mech.* **2010**, *661*, 482.

[14] C. Kloss, C. Goniva, A. Hager, S. Amberger, S. Pirker, *Prog. Comput. Fluid Dy.* **2012**, *12*, 140.

[15] L. Lu, X. Gao, T. Li, S. Benyahia, *Ind. Eng. Chem. Res.* **2017**, *56*, 13642.

[16] Y.-Q. Zhuang, X.-M. Chen, Z.-H. Luo, J. Xiao, *Comput. Chem. Eng.* **2014**, *60*, 1.

[17] M. J. Andrews, P. J. O'Rourke, *Int. J. Multiphas. Flow* **1996**, *22*, 379.

[18] D. M. Snider, *J. Comput. Phys.* **2001**, *170*, 523.

[19] A. S. Berrouk, C. Pornsilph, S. S. Bale, Y. Du, K. Nandakumar, *Energ. Fuel.* **2017**, *31*, 4758.

[20] F. Fotovat, A. Abbasi, R. J. Spiteri, H. de Lasa, J. Chaouki, *Powder Technol.* **2015**, *275*, 39.

[21] L. Yan, C. J. Lim, G. Yue, B. He, J. R. Grace, *Bioresource Technol.* **2016**, *221*, 625.

[22] The OpenFOAM Foundation, *OpenFOAM v5 User Guide*, **2017**.

[23] Z. Shang, H. Liu, "Simulating Multiphase Flows in Porous Media Using OpenFOAM on Intel Xeon Phi Knights Landing Processors," in *Proceedings of the Practice and Experience in Advanced Research Computing 2017 on Sustainability, Success and Impact*, PEARC17, ACM, New York **2017**, 47:1–47:7.

[24] J. L. Hernandez, *Influence of Drag Laws on Segregation and Bubbling Behavior in Gas-Fluidized Beds*, PhD thesis, University of Colorado at Boulder, Boulder, CO **2008**.

[25] S. Karimipour, T. Pugsley, *Powder Technol.* **2012**, *220*, 63.

[26] D. M. Snider, P. J. O'Rourke, M. J. Andrews, *Int. J. Multiphas. Flow* **1998**, *24*, 1359.

[27] P. J. O'Rourke, D. M. Snider, *Chem. Eng. Sci.* **2010**, *65*, 6014.

[28] P. J. O'Rourke, D. M. Snider, *Chem. Eng. Sci.* **2012**, *80*, 39.

[29] U. Olsbye, S. Svelle, K. P. Lillerud, Z. H. Wei, Y. Y. Chen, J. F. Li, J. G. Wang, W. B. Fan, *Chem. Soc. Rev.* **2015**, *44*, 7155.

[30] A. T. Najafabadi, S. Fatemi, M. Sohrabi, M. Salmasi, *J. Ind. Eng. Chem.* **2012**, *18*, 29.

[31] N. Hadi, A. Niaei, S. R. Nabavi, A. Farzi, M. Navaei Shirazi, *Chem. Biochem. Eng. Q.* **2014**, *28*, 53.

[32] B. Jiang, X. Feng, L. Yan, Y. Jiang, Z. Liao, J. Wang, Y. Yang, *Ind. Eng. Chem. Res.* **2014**, *53*, 4623.

[33] S. Sun, J. Li, *Chem. Eng. Res. Des.* **2014**, *92*, 2083.

[34] M. Wen, J. Ding, C. Wang, Y. Li, G. Zhao, Y. Liu, Y. Lu, *Micropor. Mesopor. Mat.* **2016**, *221*, 187.

[35] J. F. Haw, D. M. Marcus, *Top. Catal.* **2005**, *34*, 41.

[36] M. J. Luo, H. Y. Zang, B. Hu, B. H. Wang, G. L. Mao, *RSC Adv.* **2016**, *6*, 17651.

[37] X. Yuan, H. Li, M. Ye, Z. Liu, *Chem. Eng. J.* **2017**, *329*, 35.

[38] Y. Wei, C. Yuan, J. Li, S. Xu, Y. Zhou, J. Chen, Q. Wang, L. Xu, Y. Qi, Q. Zhang, Z. Liu, *ChemSusChem* **2012**, *5*, 906.

[39] D. Chen, H. P. Rebo, K. Moljord, A. Holmen, *Stud. Surf. Sci. Catal.* **1997**, *111*, 159.

[40] L. Ying, X. Yuan, M. Ye, Y. Cheng, X. Li, Z. Liu, *Chem. Eng. Res. Des.* **2015**, *100*, 179.